Journal of Civil Engineering Inter Disciplinaries
Volume 2 | Issue 2

Research Article Open Access

Buckling Bearing Capacity of Steel Plate in Steel-Concrete-Steel Sandwich Composite Tower under Axial Compression

Yu Hang. WANG [a], Guo Bing. LU [a], Shu Qi. WANG [a] and Ji Ke. TAN [a*]

[a]School of Civil Engineering, Chongqing University, Chongqing, China

***Corresponding author:** Ji Ke. TAN, School of Civil Engineering, Chongqing University, Chongqing, China, Email: tjk23@sina.com*

Citation: Yu Hang W, Guo Bing L, Shu Qi W and Ji Ke T (2021) Buckling Bearing Capacity of Steel Plate in Steel-Concrete-Steel Sandwich Composite Tower under Axial Compression. J Civil Engg ID 2(2):1-6.

Received Date: February 14, 2021; **Accepted Date:** February 24, 2021; **Published Date:** April 05, 2021

Abstract

In order to solve the problem that the traditional steel tower is prone to collapse due to local buckling under axial compression, considering the principle of composite structures, a new type of steel-concrete-steel (SCS) sandwich composite tower for wind power tower structure is proposed in this paper. In order to study the buckling bearing capacity of steel plate in SCS sandwich composite tower, three specimens were designed considering the key parameters of the curvature (the reciprocal of radius) and the spacing-to-thickness ratio (the ratio of vertical stud spacing and surface steel plate thickness). The inner and outer steel plates are connected to the concrete by the studs, and the concrete does not directly bear the vertical load and only provides brace to the steel plates. The specimens were tested under axial compression, the failure modes and load-displacement curves of the specimens were achieved. The test results show that: (1) local buckling failure between studs occurs in all specimens (2) when the spacing-to-thickness ratio is 65, the buckling bearing capacity of the specimen with an inner steel plate curvature of 0.001 is 73% higher than that of the flat steel plate specimen; (3) when the inner steel plate with a curvature of 0.001, the spacing-to-thickness ratio changes from 109 to 65, and the buckling capacity of the specimen increases by 24%.

Keywords: Axial Compression; Buckling Capacity; Curvature; Spacing-To-Thickness Ratio; Steel-Concrete-Steel Sandwich Composite Tower

1. Introduction

Wind energy is a kind of clean renewable energy; wind power generation is the most widely used and the fastest-growing new energy generation technology. As a main force suffering structure in the wind turbine, the tower not only supports the weight of nacelle and rotor, but also bears the wind load and dynamic load. Therefore, the tower plays an important role in the stable operation of the whole machine. At present, steel tower is the most common form of large wind power tower, which is prone to collapse due to local buckling under the action of complex loads, as shown in Fig. 1[1]. In order to solve the problem that the traditional steel tower is prone to collapse due to local buckling under axial compression, considering the principle of composite structures, a new type of steel-concrete-steel (SCS) sandwich composite tower for wind power tower structure is proposed in this paper, as shown in Fig. 2. The inner and outer steel plates of SCS sandwich composite tower are connected to the concrete by the studs, giving full play to the material advantages of concrete and steel. At the same time, concrete acts as a brace for steel plates, and the arrangement of studs makes the buckling of steel plates occur only within the spacing between studs, which greatly improves the buckling bearing capacity of steel tower.

Figure 1: Collapse of steel tower due to local buckling

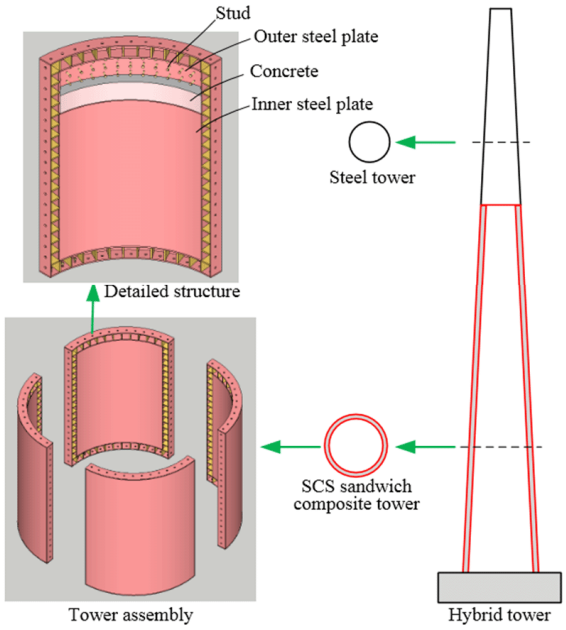

Figure 2: Schematic diagram of SCS sandwich composite tower

A great number of experimental and theoretical studies on the buckling performance of SCS sandwich composite structure could be found in the literature. Based on the existing experimental data and finite element analysis, Zhang et al. [2] gave the slenderness ratio limit of steel plate in SCS sandwich composite wall to prevent steel plate buckling before yield. Based on the elastic thin plate theory and the principle of energy standing value, Nie et al. [3] derived the critical load of local instability of composite plate, and obtained the calculation formulas of maximum stud spacing and minimum concrete plate thickness under axial compression. Huang et al. [4] conducted an experimental study on the axial compression performance of SCS sandwich composite wall in filled with ultra-lightweight cementitious composite material and proposed an improved bearing capacity calculation formula based on Euro code 4 and AISC 360. Liu et al. [5] and zhang et al.[6] respectively carried out axial compression tests on SCS sandwich composite walls with different spacing-to-thickness ratio, and gave the formula of the spacing-to-thickness ratio limit to prevent steel plate local elastic buckling. Yang et al. [7] conducted axial compression tests on 10 SCS sandwich composite walls. Considering the arrangement of studs and spacing-to-thickness ratio as variables, a theoretical model based on euler equation to predict the buckling stress of steel plates was proposed. Ding et al. [8] conducted axial compression tests on SCS sandwich composite walls only loaded on concrete, and studied the influence of steel plate thickness, stud length and angle between stud head and wall axis on bearing capacity.

The above researches mainly focus on the load cases of SCS sandwich composite structure where the axial force only loaded on the concrete or the axial force loaded on the concrete and steel. No study has been made on the load case where the axial force only loaded on the steel, and no one has studied the effect of curvatureon the buckling bearing capacity of steel plate in SCS sandwich composite structure. Therefore, three specimens were designed considering the key parameters of the curvature (the reciprocal of radius) and the spacing-to-thickness ratio (the ratio of vertical stud spacing and surface steel plate thickness). Among them, the inner and outer steel plates are connected to the concrete by the studs, and the axial load is only applied on steel plates, while the concrete only provides a brace to the steel plates, so as to investigate the buckling bearing capacity of steel plate in SCS sandwich composite tower.

2. Test Programe

2.1 Specimen design

Three specimens were designed in this test, and the section centroid of the steel plate coincided with that of the end plate. SP2 was the compared specimen, SP1 was aimed to investigate the effect of the spacing-to-thickness ratio, and SP3 was aimed to investigate the effect of the curvature. The detailed parameters of specimens are listed in Table 1, and the geometric structures of specimens are presented in Fig. 3 and Fig. 4.

Table 1: Detailed parameters of specimens

Specimen No.	t(mm)	h_t(mm)	R_i(mm)	S_i(mm)	S_o(mm)	S_v(mm)	S_v/t -
SP1	2.30	103.78	1000	244	269	250	109
SP2	2.30	103.00	1000	147	161	150	65
SP3	2.28	103.72	∞	150	150	150	65

Where: t-thickness of the steel plate; h_t-thickness of the specimen; R_i-radius of the inner steel plate; S_i-spacing of studs on the inner steel plate along the arch direction; So-spacing of studs on the outer steel plate along the arch direction; S_v-spacing of studs on the inner and outer steel plate along the height direction.

To ensure that the axial force would not be transferred to the concrete infill, a polytetrafluoroethylene (PTFE) layer was added between the steel plate and the concrete infill, and form boards with a thickness of 10 mm were placed between the adjacent studs. In order to accurately control the height of each layer of concrete and facilitate the spread of form boards, a 50mm × 50mm hole was opened at the design height of the side plate of form boards. After the concrete was poured, the hole was welded with small steel plate.

The grade of the concrete infill was C30, and the characteristic 28-day cubic strength of concrete was 37.3MPa. The material grade of steel plates was Q235B, and the measured yield strength of steel plates was 332.33 MPa, the ultimate strength was 455.33 MPa.

2.2 Specimen processing

Auxiliary stiffeners were welded on the outside of steel plate to prevent deformation, and the studs were welded on the inside of steel plate (Fig. 5(a)). After a PTFE layer was pasted on steel plate (Fig. 5(b)), the steel plates and end plates were welded together to complete the processing of steel specimen. As shown in Fig. 5(c), form boards with a thickness of 10 mm were placed between the adjacent studs when pouring concrete. The concrete was poured through holes reserved on the upper end plate, and workers compacted from bottom to top with a vibrating rod. Finally, welding the small steel plates (Fig. 5(d)) at the hole of the side plate finished the specimen processing.

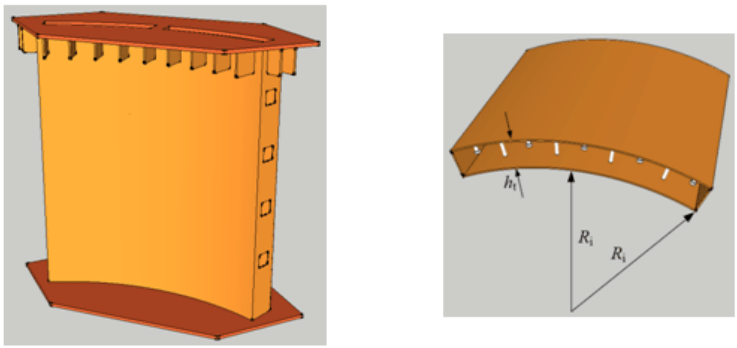

(a) Overall diagram (b) Inner diagram

Figure 3: Geometric structures of specimens

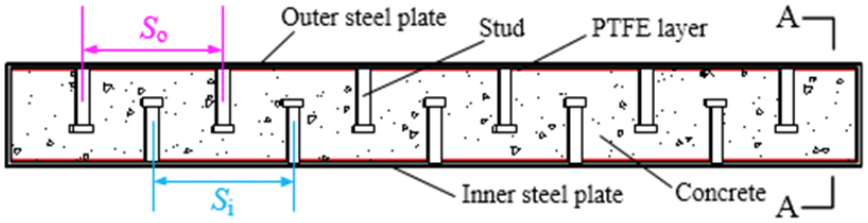

(a) Section diagram of flat plate specimen

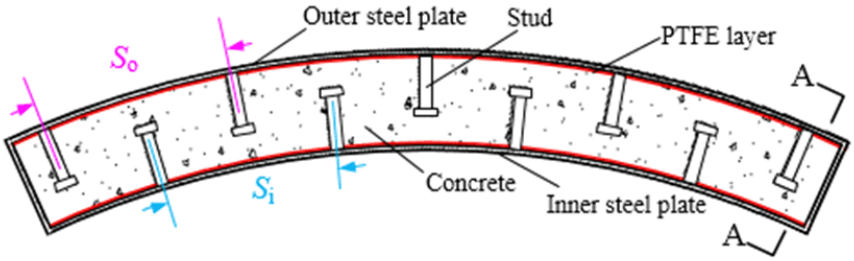

(b) Section diagram of curved plate specimen

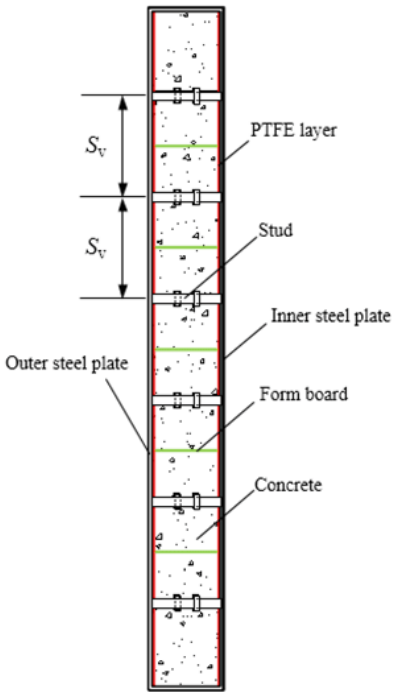

(c) A-Asection

Figure 4: Inner structure of specimens

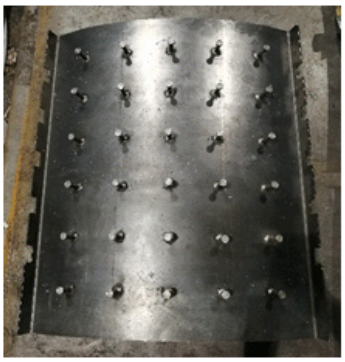

(a) Welding studs

(b) Pasting PTFE layer

(c) Pouring concrete

(d) Welding small plates

Figure 5: Specimen processing

2.3 Test equipment and measurement scheme

The compression tests were conducted by servo controlled electro hydraulic testing machine in the Structural Laboratory of Xi'an University of Architecture and Technology. The test equipment and measurement scheme are shown in Fig. 6.The axial force of the specimen was measured by the force sensor of the device, and the axial displacement was measured by Linear Variable Differential Transformer (LVDT) displacement meter arranged symmetrically at the center of the inner and outer steel plates. Monotonic axial loading was applied in the test, which could be divided into two stages: preloading and formal loading. The main function of preloading was to check whether the specimen was uniformly stressed and whether the displacement meter worked properly. The load of preloading was 10%nominal bearing capacity (equal to $f_y A_s$). After the preloading, the formal loading was loaded by displacement control. When the specimens were significantly deformed and severely damaged, the tests were stopped.

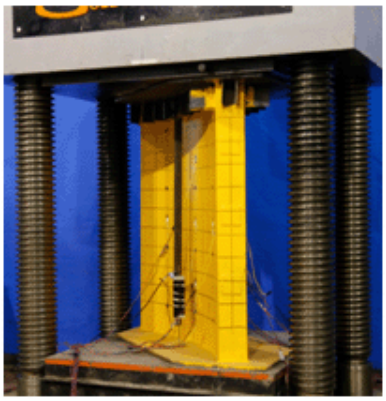

(a) Test equipment

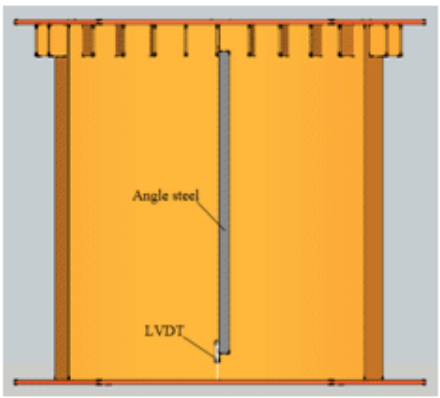

(b) Measurement scheme

Figure 6: Test equipment and measurement scheme

3. Test Phenomena and Failure Mode

Before the peak load of specimen SP2, the first horizontal interval of the second row of studs on the inner steel plate began to buckle, and the steel plate buckled below the first row of studs on the upper right of outer steel plate. After the peak load of 955.3kN, the curve at the upper right of outer steel plate was pulled through. With the increase of the load, the curve at the second row of inner steel plate was pulled through between the horizontal studs. When the load continued to increase, the curve on the inner and outer steel plate was pulled through at the left and right side plate. The final failure mode of specimen SP2 is shown in Fig.7.

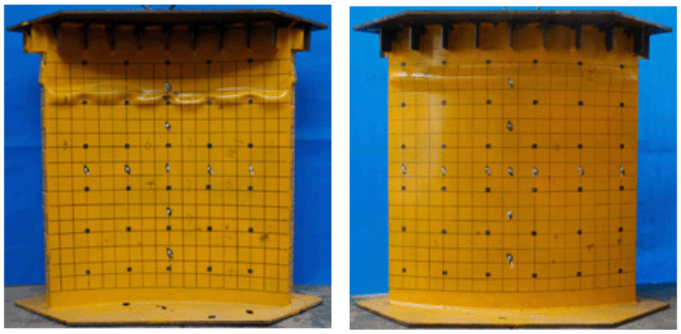

(a) Inner steel plate (b) Outer steel plate

Figure 7: Failure mode of specimen SP2

The vertical stud spacing of SP1 decreased. Before the peak load, the inner steel plate began to buckle between the studs along the diagonal, followed by the steel plate buckledbelow the first row of studson the upper left of outer steel plate. After the peak load of 771.4kN, the curve at the upper left of outer steel plate was pulled through, and three intervals of studs on the upper left of inner steel plate buckled.When the load continued to increase, the upper right of inner steel plate began to buckle, and the steel plate on the top of the left plate and right plate buckled. The final failure mode of specimen SP1 is shown in Fig. 8.

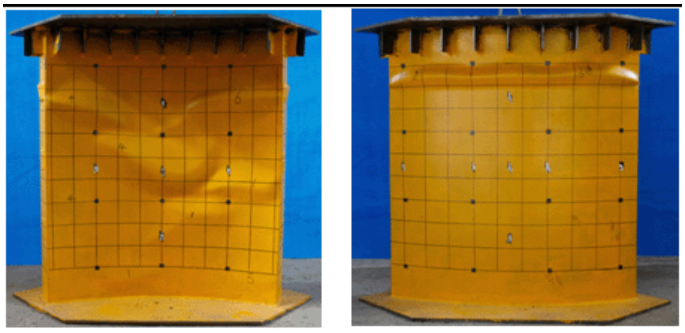

(a) Inner steel plate (b) Outer steel plate

Figure 8: Failure mode of specimen SP1

Specimen SP3 was a flat steel plate specimen. Before the peak load, the long curve occurred on the lower middle of outer steel plate. After the peak load of 550.3kN, the long curve occurred on the lower middle of inner steel plate. When the load continued to increase, the curve on the inner and outer steel plate was pulled through at the left and right side plate. The final failure mode of specimen SP3 is shown in Fig. 9.

The test phenomenon shows that local buckling failure between the studs occurred on the steel plates of all specimens. The arrangement of studs limited the buckling failure of steel plates only occur between adjacent studs. Compared with the flat steel plate specimen, the curved steel plate specimen had a certain out-of-plane stiffness, thus the buckling half-wavelength of inner and outer steel plates decreased. When the inner steel plate with a curvature of 0.001, the spacing-to-thickness ratio changed from 109 to 65, the buckling half-wavelength of inner steel plate decreased.

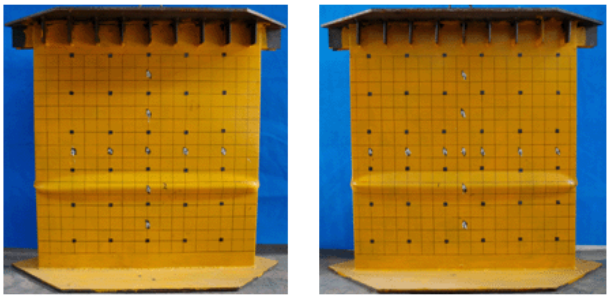

(a) Inner steel plate (b) Outer steel plate

Figure 9: Failure mode of specimen SP3

4. Buckling Bearing Capacity

The buckling bearing capacity (maximum bearing capacity) of the specimens is listed in table 2, and the load-displacement curves are shown in Fig. 10.It can be seen that when the spacing-to-thickness ratio is 65, the buckling bearing capacity of the specimen with an inner steel plate curvature of 0.001 is 73% higher than that of the flat steel plate; when the inner steel plate with a curvature of 0.001, the spacing-to-thickness ratio changes from 109 to 65, and the buckling capacity of the specimen increases by 24%.

When the spacing-to-thickness ratio is constant, the buckling bearing capacity of the curved steel plate specimen because of theout-of-plane stiffness is higher than that of the flat steel plate specimen. The arrangement of the studs limits the buckling failure of the steel plates only occur between adjacent studs. The decrease of the spacing-to-thickness ratio means the decrease of the distance between studs. In this way, the buckling half-wavelength will be reduced accordingly. The decrease of the buckling half-wavelength is converted to the increase of buckling bearing capacity.

Table 2: Buckling bearing capacity of specimens

Specimen No.	R_i(mm)	S_v/t	P_u(kN)
SP1	1000	109	771.4
SP2	1000	65	955.3
SP3	∞	65	550.3

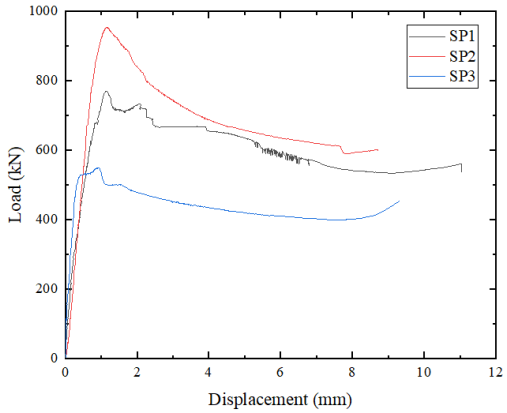

Figure 10: Load-displacement curve

5. Conclusion

In this paper, the axial compression tests of three steel-concrete-steel sandwich composite tower specimens only loaded on steel were successfully conducted, and the following conclusions could be obtained through the observation of experimental phenomena and the analysis of test results:

(1) Local buckling failure between studs occurs on the steel plates of all specimens. Compared with the flat steel plate specimen, the curved steel plate specimen has a certain out-of-plane stiffness, thus the bucklinghalf-wavelength of inner and outer steel plates decreases. When the inner steel plate with a curvature of 0.001, the spacing-to-thickness ratio changes from 109 to 65, the bucklinghalf-wavelength of inner steel plate decreases. The decrease of the buckling half-wavelength is converted to the increase of buckling bearing capacity.

(2) When the spacing-to-thickness ratio is 65, the buckling bearing capacity of the specimen with an inner steel plate curvature of 0.001 is 73% higher than that of the flat steel plate. When the inner steel plate with a curvature of 0.001, the spacing-to-thickness ratio changes from 109 to 65, and the buckling capacity of the specimen increases by 24%.

Acknowledgements

The research is supported by the Project of Fok Ying Tung Education Foundation (171066) 、National Natural Science Foundation of China (51890902) and Chongqing Science and Technology Bureau (cstc2019jcyj-zdxm0099).

References

1. Pan FS, Wang FW, Ke ST, Tang G. Buckling analysis and stability design of wind turbine tower with geometic imperfections. Acta Energiae Solaris Sinica. 2017,0254-0096(2017)10-2659-06. (in Chinese)
2. Zhang K, Varma AH, Malushte SR, Gallocher S. Effect of shear connectors on local buckling and composite action in steel concrete composite walls. Nuclear Engineering and Design. 2014;269:231-239.
3. Nie JG, Li FX. Study on the Stability of Steel-Concrete CompositePlates under Uniaxial Compressed Load. China Railway Science. 2009;30(6):27-32. (in Chinese)
4. Huang Z, Liew JYR. Compressive resistance of steel-concrete-steel sandwich composite walls with J-hook connectors. Journal of Constructional Steel Research. 2016;124:142-162.
5. Liu YB, Wang S, Liu JB, Niu Q. Experimental study on local buckling behavior of composite walls with double steel plates and filled concrete. Journal of Hohai University (Natural Sciences). 2017;45(4):317-323. DOI: 10.3876/j.issn.1000-1980.2017.04.006.(in Chinese)
6. Zhang YJ, Li XJ, He QM, Yan X. Experimental study on local stability of composite walls with steel plates and filled concrete under concentric loads. China Civil Engineering Journal. 2016;49(1):62-68. (in Chinese)
7. Yue Y, Liu J, Fan J. Buckling behavior of double-skin composite walls: An experimental and modeling study. Journal of Constructional Steel Research. 2016;121:126-135.
8. Ding LT, Seismic behavior of double steel plate-intersect studs-concrete composite shear wall. Institute of Engineering Mechanics, CEA. 2014. (in Chinese)